Rare Metal Materials and Engineering
Volume 53, Issue 6, June 2024
Available online at www.rmme.ac.cn

Science Press

Cite this article as: Zhang Wenbin, Yang Haijuan, Liu Cuirong, et al. Numerical Simulation and Experiment Analysis of N6/45# Composite Plate Prepared by Explosive Welding[J]. Rare Metal Materials and Engineering, 2024, 53(06): 1592-1600. DOI: 10.12442/j.issn.1002-185X.20230600.

ARTICLE

Numerical Simulation and Experiment Analysis of N6/45# Composite Plate Prepared by Explosive Welding

Zhang Wenbin[1], Yang Haijuan[1], Liu Cuirong[1,2], Li Yan[1,2], Shi Aizun[1]

[1] School of Material Science and Engineering, Taiyuan University of Science and Technology, Taiyuan 030024, China; [2] Preparatory Department, Modern College of Humanities and Sciences, Shanxi Normal University, Linfen 041000, China

Abstract: In order to reduce cost and to fully utilize the excellent corrosion resistance of nickel materials, pure nickel N6 with thickness of 1 mm was selected as the flyer plate, and the medium carbon steel 45# with thickness of 3 mm was used as the base plate for explosive welding tests. The dynamic parameters were calculated through the explosive welding window, and the interface bonding morphology and elements were analyzed by metallographic optical microscope and scanning electron microscope. The mechanical properties of the composite plate were tested through shear tests, and the explosive welding process was simulated by AUTODYN. Results indicate that there is a boundary effect near the explosion point, and the bonding interface along the explosion welding direction changes from the flat state to the stable wavy interface. The thickness of the element diffusion layer near the interface is 20 μm, and the wavy diffusion layer increases the bonding area, which is conducive to the metallurgical bonding. The shear strength of the composite plate reaches 325.5 MPa. Numerical simulation analysis results demonstrate that the simulated interface morphology is consistent with the experiment results. The simulation results show that the velocity and plastic deformation degree of the characteristic points are basically consistent with the experimental results.

Key words: explosive welding; N6/45# composite plate; welding window; numerical simulation

Explosive welding is a widely used welding technique for metal composite bonding, which can achieve the preparation of double- or multi-layer metal plates and pipes. Bimetallic composite plates are the commonest products and they can satisfy the customized industrial requirements. Another advantage of explosive welding, as a cutting-edge welding technique, is that it can prepare metal composites whose components have significant differences in physical properties and inferior metallurgical incompatibility. Usually, the metals with low and high prices are combined by explosive welding to obtain excellent physical and chemical properties and to reduce cost[1–6]. The principle of explosive welding is to use the detonation energy released by the explosion of explosives to accelerate the base plate, causing high-speed impact of metals and achieving metallurgical bonding in the collision zone at the metal interface.

The explosive welding process involves the intersection of multiple disciplines, and complex physical and chemical changes occur in a very short explosion time. Thus, appropriate explosive welding process parameters have been widely researched. Currently, the theoretical research on explosive welding is not yet perfect, and only explosive welding window can provide a reasonable range of process parameters[7]. With the development of computer technology, numerical simulation has become a commonly used research method for explosive welding. Finite element software ANSYS, AUTODYN, and other platforms for numerical simulation provide reliable basis for the favorable experiments. Zeng et al[3] simulated the explosive welding process by smoothed particle hydrodynamics (SPH) method and obtained different welding interfaces by changing experiment parameters, such as collision angle and collision point velocity, therefore significantly influencing the mechanical properties of composite plate. Wang et al[8] used SPH method in AUTODYN software to simulate the Ti/Cu explosion welding experiment, which used a stepped method

Received date: September 23, 2023
Foundation item: National Key Research and Development Program (2018YFA0707305); Basic Research Program of Shanxi Province (202203021221149); Major Science and Technology Projects of Shanxi Province (202101120401008)
Corresponding author: Li Yan, Ph. D., Associate Professor, School of Material Science and Engineering, Taiyuan University of Science and Technology, Taiyuan 030024, P. R. China, E-mail: yanli1988@tyust.edu.cn

to arrange the base plate. It is found that with the increase in spacing, the melting zone is enlarged, and different types of intermetallic compounds appear. Based on the number of observation points in the jet, it is found that the main source of the jet is titanium plate. Tian et al[9] simulated the explosive welding of Al/Fe composite by AUTODYN software and found that the welding quality is related to the collision speed. When the collision speed is too low or too high, explosive welding cannot well combine the metals. When the collision speed is 600 m/s, optimal welding quality can be achieved. Li et al[10] simulated the formation process of Fe/Fe interface during explosive welding based on SPH method. It is concluded that explosive welding is a combination of fusion welding, diffusion welding, and pressure welding. Wu et al[11] applied SPH-finite element method coupling algorithm to simulate several typical explosive composite plates, including Ti/Fe, stainless steel/Fe, Cu/Fe, and Ti/Al, and studied the effects of thickness and spacing between the flyer plate and base plate on the interface temperature, pressure, and microstructure. Results show that with the increase in spacing and thickness of flyer plate, the interface temperature, pressure, and waveform size are all increased.

Pure nickel N6 is a silver white metal with excellent corrosion resistance in heavy non-ferrous metals, especially in caustic environment. It has excellent comprehensive performance in complex environment and is widely used in evaporator, alkali storage tank, heater, and pipeline in the alkali industry[12–15]. Steel 45# has low cost and a wide range of applications in industrial production due to its good corrosion resistance and wear resistance in the air. However, nickel-based materials are limited and thereby expensive, restricting their application. Therefore, the nickel-related alloys become the research focus[16]. In this research, the pure nickel N6 was used as the flyer plate and the medium carbon steel 45# was used as the substrate for explosive welding to prepare N6/45# composite plates. Experiment analysis of interface bonding morphology and element distribution was conducted by optical microscope (OM) and scanning electron microscope (SEM) coupled with energy dispersive spectroscope (EDS). The mechanical properties of the composite plate were tested through shear testing. In order to balance the calculation accuracy and efficiency, AUTODYN software was adopted in this research. SPH method was used for the flyer plate and base plate, and arbitrary Lagrangian Euler (ALE) method was used for explosive simulation experiments. The analysis of the simulation results provides theoretical reference for the preparation of N6/45# composite plate.

1 Explosion Welding Window

In the process of explosive welding, it is necessary to select the correct process parameters. Explosive welding window can provide a reasonable range to obtain qualified composite plates. As shown in Fig. 1, the explosion welding window is generally composed of collision point movement velocity V_c, collision velocity V_p, and dynamic collision angle β. The geometric relationship among the three components is shown in Eq.(1), as follows:

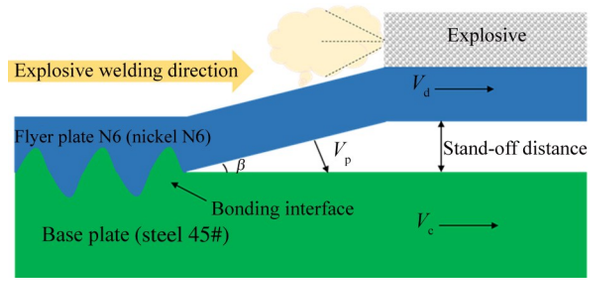

Fig.1 Schematic diagram of explosive welding process

$$V_p = 2V_c \sin\frac{\beta}{2} \tag{1}$$

When the substrate is installed parallel to the composite plate, the detonation velocity (V_d) of the explosive sacisfies V_d=V_c.

The most commonly used explosive welding window is composed of V_p and V_c coordinate systems, which are surrounded by four boundary lines: upper limit, flow limit, sound speed limit, and lower limit.

1.1 Sound speed limit of explosive welding

The sound speed limit can limit the energy during the formation of the jet. In order to ensure the jet formation, Walsh et al[17] proposed that the movement speed V_c of the collision point should be less than the sound speed of material. During explosive welding, V_c is taken as the minimum volume sound speed in the material. Therefore, the sound speed limit can be calculated by Eq.(2), as follows:

$$V_{c_{max}} = \min(C_1, C_2) \tag{2}$$

where C_1 and C_2 are the sound velocities of the substrate and the composite plate, respectively.

1.2 Flow limit of explosive welding

The flow limit is the condition where jet is generated during collision. Only when the collision point movement velocity V_c at the collision point exceeds the minimum value $V_{c_{min}}$, jet can be generated. Otherwise, the junction zone can only be a straight junction. The value of the flow limit can be calculated by Eq.(3)[18], as follows:

$$V_{c_{min}} = \sqrt{\frac{2Re(H_{Vf} + H_{Vb})}{\rho_f + p_b}} \tag{3}$$

where Re is the Reynolds number; H_{Vb} and H_{Vf} are the Vickers hardness of the base plate and the flyer plate, respectively; ρ_b and ρ_f correspond to the density of the base plate and the flyer plate, respectively.

1.3 Lower limit of explosive welding

For dissimilar materials, the collision velocity V_p should be greater than the critical collision velocity $V_{p_{min1}}$ for jet generation to ensure the success of explosive welding. The lower limit of the explosive welding window can be calculated by the equivalent normal shock wave model[19], as follows:

$$P_{min} = \max(\rho_1 c_1 \frac{V_{p_{min1}}}{2}, \rho_2 c_2 \frac{v_{p_{min2}}}{2}) \tag{4}$$

$$V_{p_{min}} = p_{min}\left(\frac{1}{\rho_1 c_1} + \frac{1}{\rho_2 c_2}\right) \quad (5)$$

where P_{min} is the minimum collision pressure between the flyer plate and the base plate; $V_{p_{min1}}$ and $V_{p_{min2}}$ are the lower limits of collision velocity for the flyer plate and the base plate, respectively.

1.4 Upper limit of explosive welding

The upper limit of explosive welding is the maximum energy limit when the composite plate collides with the substrate. If the collision speed is too high, it is easy to store too much energy in the bonding interface area, leading to non-bonding state of interface and excessive melting. The upper limit of explosive welding can be calculated by Eq. (6) [20], as follows:

$$V_{p_{max}} = \frac{1}{N}\frac{(T_m C_0)^{\frac{1}{2}}}{V_c}\frac{\lambda C_0 C_p}{\rho h}^{\frac{1}{4}} \quad (6)$$

where N is the material constant of 0.1; T_m is the melting point; C_0 is the sound velocity of the flyer plate; C_p is the specific heat capacity; λ is the thermal conductivity; ρ is the material density; h is the thickness of the flyer plate.

1.5 Selection of optimal parameters for explosive welding window

According to Eq. (1 – 6), the welding explosive process parameters are sound speed limit $V_{c_{max}}$=5200 m/s, flow limit $V_{c_{min}}$=2095.7 m/s, lower limit $V_{p_{max}}$=296.1 m/s, and the upper limit $V_{p_{max}}$=2062.5 m/s. Based on these parameters, the explosive welding window can be obtained, as shown in Fig.2.

The explosive welding window provides the exercisable range of parameters for explosive welding, but not all parameters within this range can achieve the optimal welding effect. Therefore, it is necessary to select the approximate parameters for optimal welding quality.

The optimal collision point movement speed can be determined by the sound speed limit and flow limit, as follows:

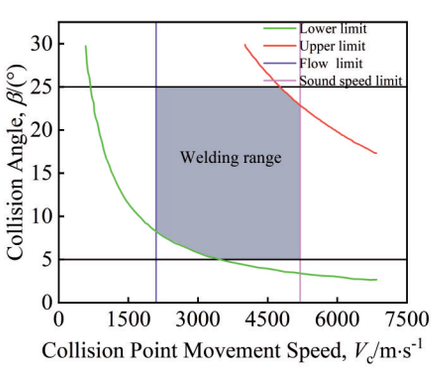

Fig.2 Explosion welding window for N6/45# composite plate

$$\begin{cases} V_c = V_{c_{min}} + 200 & V_{c_{min}} < 2000 \text{ m/s} \\ V_c = V_{c_{min}} + 100 & 2000 < V_{c_{min}} < 2500 \text{ m/s} \\ V_c = V_{c_{min}} + 500 & V_{c_{min}} > 2000 \text{ m/s} \end{cases} \quad (7)$$

The optimal collision speed between the base plate and the flyer plate can be determined based on the upper and lower limits in the explosive welding window, as expressed by Eq.(8)[21], as follows:

$$V_p = V_{p_{min}} + 0.1(V_{p_{max}} - V_{p_{min}}) \quad (8)$$

The distance between the flyer plate and the base plate provides space for the movement of flyer plate during explosive welding. The distance between the flyer plate and base plate can be calculated by Eq.(9), as follows:

$$H = 0.2(\delta + h_f) \quad (9)$$

where δ is the thickness, H is the distance between the flyer plate and the base plate, and H_f is the thickness of the flyer plate.

According to the abovementioned formulae, the optimal parameters for explosive welding are as follows: the spacing between the flyer plate and the base plate is 2 mm, ANFO explosive density is 850 kg/cm^3, thickness is 9 mm, charge ratio is 0.9, optimal collision angle β is 12.5°, optimal collision point movement speed V_c is 2100 m/s, and optimal collision speed V_p is 470 m/s.

2 Experiments and Results

2.1 Experiment

The size of pure nickel N6 and steel 45# was 300 mm×300 mm×1 mm and 300 mm×300 mm×3 mm, respectively. The chemical composition of nickel N6 and steel 45# is shown in Table 1.

This explosion welding experiment adopted a parallel installation method and an edge center detonation method.

After the explosion, the composite plate was cut along the direction of detonation propagation for shear strength tests, and it was also cut at different positions from the initiation point for metallographic tests. After polishing, the interface bonding morphology of the composite plate was observed by OM (VHX-2000), and the interface element analysis was conducted by SEM equipped with EDS. The size of the tensile shear specimen was determined according to GB/T6396-2008, as shown in Fig.3.

2.2 Results and analysis

2.2.1 Interface morphology

Fig. 4 shows the interface morphologies of N6/45# composite plate along the explosion direction. Fig. 4a shows the interface morphology near the initiation point. It can be seen that during the initial stage of explosion, the nickel N6 plate and steel 45# plate do not combine. Li et al[22] conducted

Table 1 Chemical composition of steel 45# and pure nickel N6 (wt%)

Material	C	Si	Mn	Cu	S	P	Cr	Mo	Ni	Fe
Steel 45#	0.43	0.25	0.55	0.02	0.024	0.013	0.05	0.09	0.02	Bal.
Nickel N6	0.01	0.13	0.03	0.008	-	-	-	-	Bal.	0.05

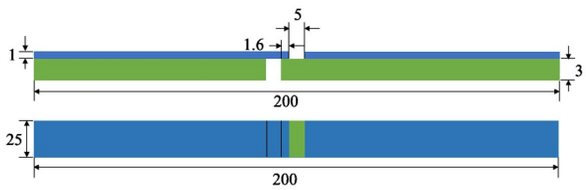

Fig.3 Schematic diagram of tensile shear specimen

in-depth analysis in Ti/Al explosion process and found similar results. These phenomena are attributed to the fact that near the initiation point, the newly ignited explosive has low energy and unstable detonation, and the detonation products are affected by sparse waves, resulting in the low-pressure state near the initiation point and the appearance of boundary effects. As shown in Fig. 4b, the bonding interface exhibits a flat morphology. At this point, the collision velocity V_p is less than the critical collision velocity $V_{p_{min}}$, resulting in the inability of jet generation and unstable bonding of the composite plate. At the location far from the initiation point, the bonding surface changes to a wavy morphology, achieving the optimal form of explosive welding. The wavy interface increases the bonding area of the two materials, enhances the mechanical meshing effect, broadens the metallurgical bonding range, and significantly improves the bonding strength[23].

Fig. 5 shows the characteristic morphologies of the vortex zone at the bonding interface. Individual vortex structures can be observed at the peak of the waveform area in Fig. 5a. The large number of whirlpool can affect the bonding strength of interface, but defects, such as voids and microcracks, usually exist at the whirlpool, reducing the possibility of defect expansion and the adverse effect on the bonding surface.

In addition, a black molten block can be observed at the whirlpool, indicating the similar degrees of plastic deformation for the flyer plate and base plate. The molten block can store a large number of defects generated by explosions, which is conducive to the bonding of atoms between metals[24–25]. As shown in Fig. 5b, it is also found that there is a trunk structure at the bonding interface. This is due to the high temperature and high pressure at the interface collision point. The jet is divided into two streams during the initial process, and the upward structure of the substrate captures the convex jet, leading to the formation of trunk structure.

2.2.2 Interface element analysis

The diffusion of elements at the interface has an important impact on the microstructure and mechanical properties of materials, creating favorable conditions for metallurgical bonding at explosive welding interfaces. EDS line scanning results of the interface are shown in Fig. 6. The white line in Fig. 6a represents the scanning path and Fig. 6b shows the distribution of Fe and Ni elements. At the bonding interface, the thickness of the diffusion layer is about 20 μm. The thermal motion of the detonation waves in explosive welding causes Brownian motion of atoms or molecules, resulting in the uniform diffusion layer.

It can be observed that Fe element diffuses from steel 45# plate to nickel N6 plate, whereas Ni element diffuses from nickel N6 plate to steel 45# plate.

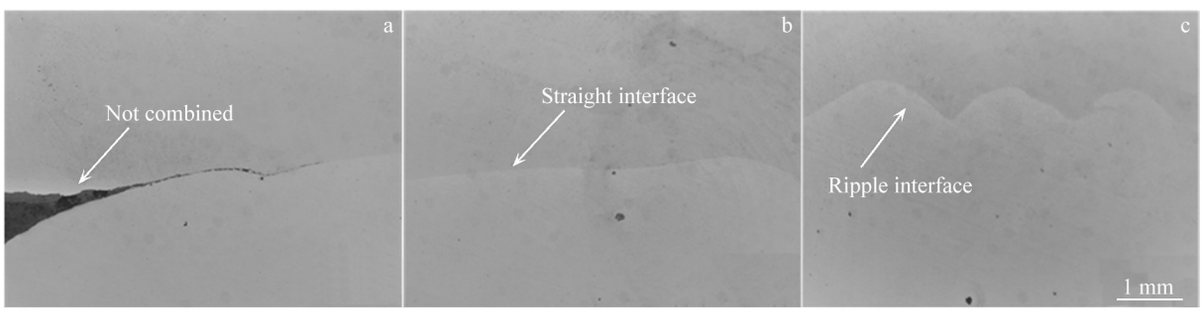

Fig.4 Interface morphologies of N6/45# composite plate along explosion direction: (a) near the initiation point; (b) bonding interface; (c) far from the initiation point

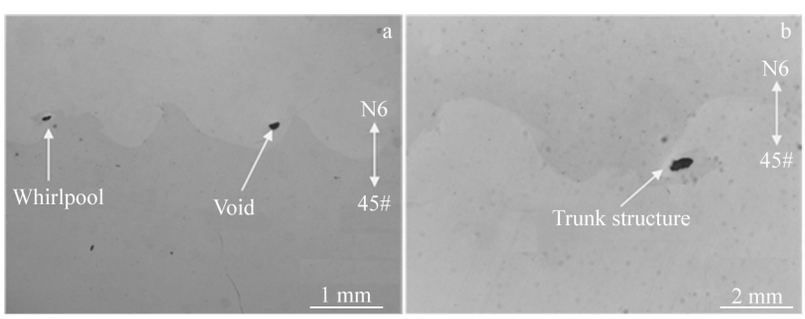

Fig.5 Characteristic morphologies of vortex zone at bonding interface: (a) whirlpool structure; (b) trunk structure

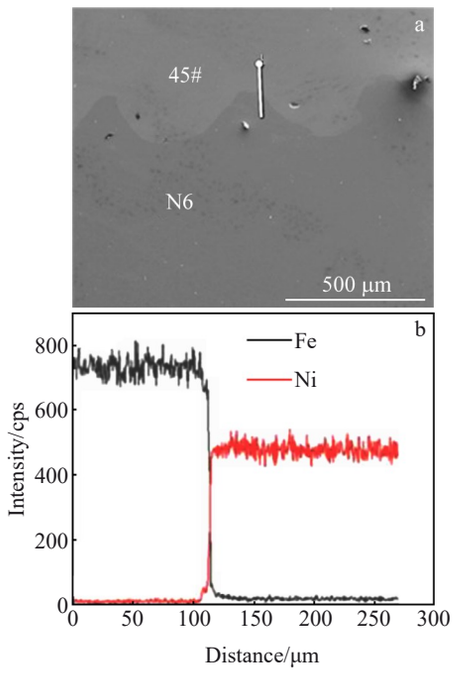

Fig.6 SEM image (a) and EDS spectra (b) of N6/45# interface

In addition, the radii of Fe and Ni atoms are 0.127 and 0.128 nm, respectively, which are almost equal. Therefore, displacement diffusion occurs, resulting in a high degree of plastic deformation at the interface, as indicated by the appearance of plastic deformation band near the interface.

2.2.3 Shear strength analysis

Shear strength is one of the important indicators to judge the welding quality of composite plates prepared by explosive welding. To test the mechanical properties of N6/45# explosive composite plate, room temperature tensile shear tests were conducted. Fig. 7 shows the shear stress-displacement curve of N6/45# composite plate, which shows shear strength of 325.5 MPa at the interface. It can be seen that the N6/45# composite plate prepared by explosive welding has high bonding strength. In addition, due to the wavy bonding interface of the N6/45# composite plate, the actual bonding area is larger than the calculated area, so the actual shear strength of the composite plate should be slightly smaller than the calculated value.

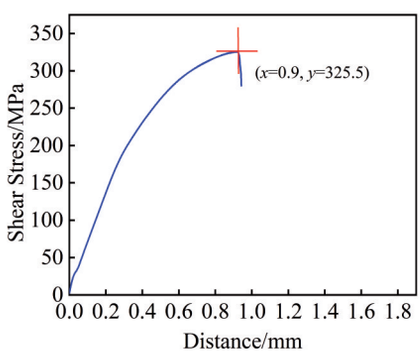

Fig.7 Shear stress-distance curve of N6/45# composite plate prepared by explosive welding

3 Simulation and Result Analysis

3.1 Numerical simulation

Due to the short duration of the explosive welding process, the relevant data during the forming process are difficult to extract from the experiment. Therefore, a two-dimensional (2D) numerical simulation was conducted through the commercial finite element software AUTODYN. The simulation of the flyer plate and the base plate used SPH method, which not only has high computational accuracy but also reflects the jet phenomenon[26]. In order to save computational cost, ALE method was used to simulate the explosives and molds. Using the edge center initiation method, gauge points 1–14 with equal distance intervals were taken on the lower surface of the composite plate and the upper surface of the substrate. The established model is shown in Fig. 8. Table 2 shows the geometric parameters of the model, and the length of the composite plate and the substrate is 30 mm.

The explosive welding process is a highly nonlinear dynamic process, and the explosive forming process involves the high strain rates and plastic hardening of materials. Therefore, the Johnson Cook constitutive equation[27] is adopted, as follows:

$$\sigma = \left(A + B\varepsilon_{\text{eff}}^{n}\right)\left(1 + C\ln\dot{\varepsilon}\right)\left(1 - T^{*m}\right) \quad (10)$$

$$T^{*m} = (T - T_{\text{room}})/(T_{\text{melt}} - T_{\text{room}}) \quad (11)$$

where σ is Von Miss flow stress; ε_{eff} represents the equivalent plastic strain; $\dot{\varepsilon}$ represents the strain rate; T_{melt} and T_{room} are the melting point of the material and room temperature, respectively; A, B, C, n, and m are constants of the material.

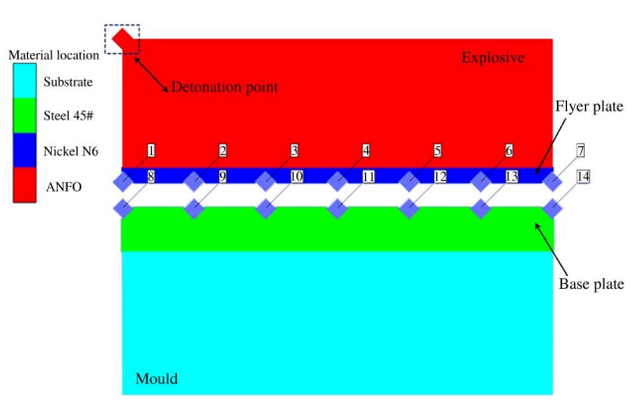

Fig.8 2D model of explosive welding for N6/45# composite plate

Table 2 Geometry parameters of 2D model of explosive welding for N6/45# composite plate (mm)

Material	Length	Height
ANFO	30	9
Nickel N6	30	1
Steel 45#	30	3
Substrate	30	10

The parameters of the two materials are shown in Table 3.

In this simulation, the Jones Wilkins Lee (JWL) equation of state for explosives was selected[28]. This equation of state can accurately describe the process of explosive expansion. JWL equation of state is shown in Eq.(12), as follows:

$$P = A(1 - \frac{\omega}{R_1 V})e^{-R_1 V} + B(1 - \frac{\omega}{R_2 V})e^{-R_2 V} + \frac{\omega E_0}{V} \quad (12)$$

where P is the pressure of the detonation product; V is the relative volume of the detonation product; E_0 is the initial specific internal energy; A, B, R_1, R_2, and ω are the parameters of the explosive. Combined with the theoretical values of the explosive welding window, Table 4 shows the results of JWL state parameters.

3.2 Simulation result analysis

The numerical simulation process is shown in Fig. 9 (excluding the explosive and mold parts), and the welding process is well reproduced. The flyer plate is accelerated to bend under the action of explosives, and then collides with the base plate, ultimately forming a composite plate. As shown in Fig. 9c, the base plate begins to produce jets. Wang et al[29] found that in the simulation of Ti/Al explosive welding, the density difference of the metals has a significant impact on the generation of jets. Due to the relatively lower density of the base plate (steel 45#), it is easier to form jet in the base plate. The generation of jet is often considered as an important condition for excellent bonding between two plates, which removes the oxide film and reduces the strain on the to-be-bonded surface, thereby promoting the bonding under high-speed collisions.

Fig. 10 shows the simulated interface morphologies of N6/45# composite plate during the welding process. It can be found that the simulation results are highly consistent with the experiment results in Fig. 4. Boundary effect appears near the initiation point. With the explosion proceeding, the interface gradually reaches the wavy bonding state from the straight flat

Table 3 Johnson-Cook model parameters of nickel N6 and steel 45#

Parameter	Nickel N6	Steel 45#
Density/kg·m^{-3}	8900	7850
Poison ratio	0.3	0.3
T_{melt}/K	2818	2723
A/MPa	163	507
B/MPa	648	320
C	0.006	0.064
m	1.44	1.06
n	0.33	0.28
T_{room}/K	298	298

Table 4 JWL state parameters of explosive welding for N6/45# composite plate

E_0/GJ	A/GJ	B/GJ	R_1	R_2	ω
2.69	34.6	2.23	3.91	1.62	0.23

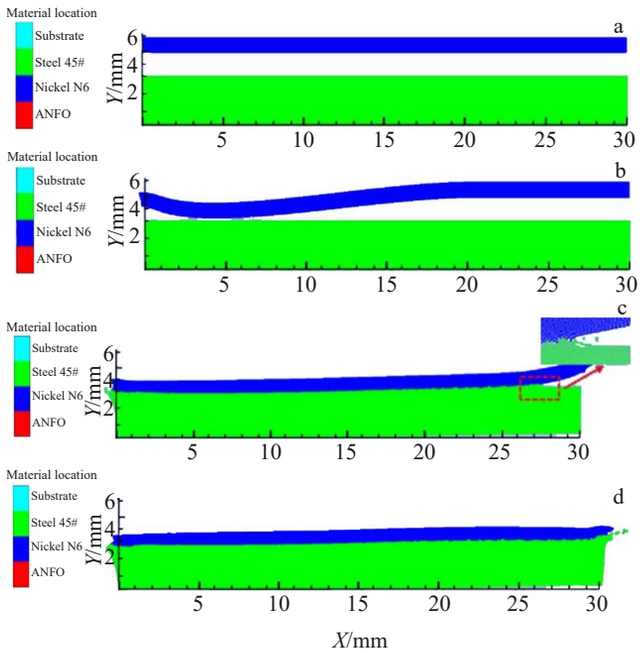

Fig.9 Simulated explosive welding process: (a) 0 ms; (b) 5.0×10^{-3} ms; (c) 1.1×10^{-2} ms; (d) 1.4×10^{-2} ms

bonding state. Explosive welding interfaces mainly include straight, wavy, and melted layer interfaces. Only the appearance of wavy interfaces can satisfy the requirements of explosive welding. The wavy interface increases the bonding area between the flyer plate and the base plate and improves the bonding strength of the composite plate.

Fig. 11 shows the velocity distribution of the N6/45# composite plate at 8.9×10^{-3} ms during explosive welding process and the velocity-time relationship at gauge point 1 – gauge point 7 along Y direction. As shown in Fig11a, the velocity near the joint surface is the highest with the jet velocity of 6500 m/s. According to Fig11b, it can be seen that the detonation velocities at the initiation point (gauge point 1) and end point (gauge point 7) are lower than those at other collision points, and stable detonation can only be achieved at the middle position of the composite plate, which is consistent with the data calculated in the explosion welding window. The maximum collision speed of gauge point 4 reaches 510 m/s. According to Fig.2, this speed is within the explosive welding window but has a small distance to the calculated optimal collision speed (470 m/s). This result indicates that the simulation and calculation results are basically consistent, and the composite plate obtained under this parameter has better quality.

Fig. 12a shows the effective plastic strain cloud map of N6/45# explosive welding at 8.9×10^{-3} ms. During the explosive welding process, a slender efficient plastic strain band is formed near the bonding interface, and the significant plastic deformation of the metal is a prerequisite for successful explosive welding. Under high temperature and high pressure, strong plastic deformation occurs at the interface, effectively improving the bonding force between interface atoms,

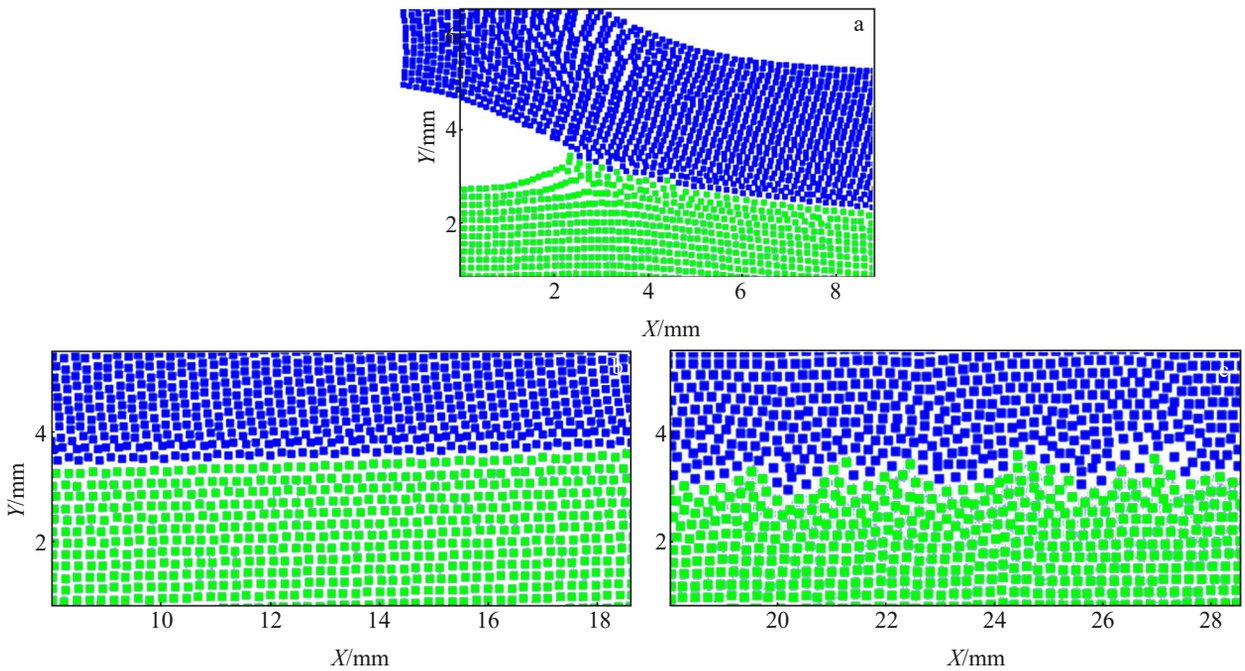

Fig.10 Simulated interface morphologies of N6/45# composite plate during welding process: (a) unwelded state; (b) straight state; (c) wavy state

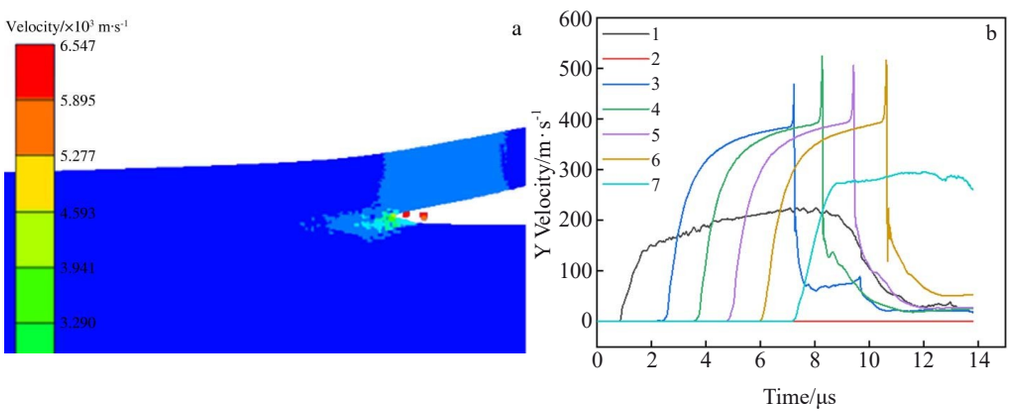

Fig.11 Velocity distribution cloud map of N6/45# explosive welding at 8.9×10^{-3} ms (a); *Y* velocity-time curves of gauge points of composite plate (b)

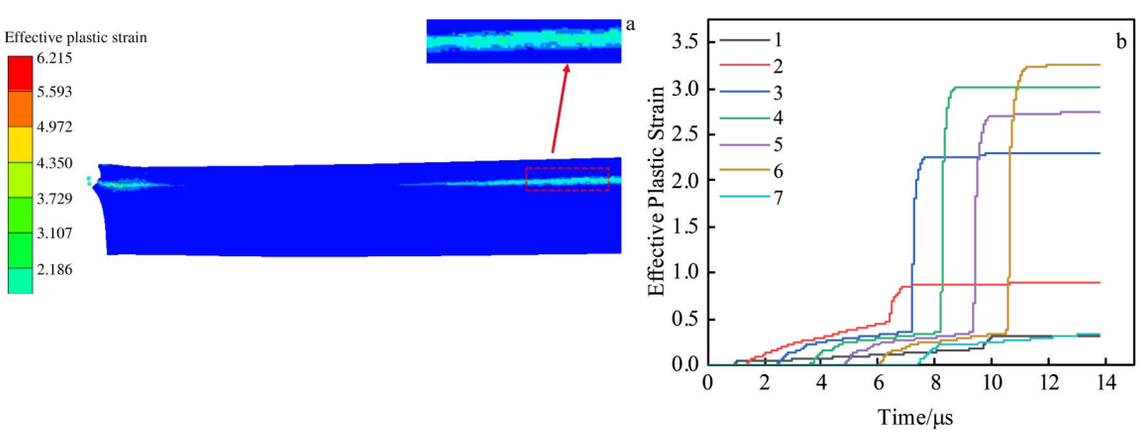

Fig.12 Effective plastic strain cloud map of N6/45# explosive welding at 8.9×10^{-3} ms (a); effective plastic strain-time curves of gauge points of composite plate (b)

promoting the atomic diffusion, and facilitating the metallurgical bonding of composite plates. As shown in Fig.12b, the effective plastic strains of the composite plate are lower at the beginning and end positions of the explosion, compared with those at other positions. Maximum effective plastic strain of 3.2 is obtained at gauge point 6. With the explosive welding further proceeding, the effective plastic strain remains stable, indicating that the plastic deformation is an irreversible process[30].

4 Conclusions

1) Appropriate explosive welding parameters for the N6/45# composite plate are obtained by the explosive welding window: the spacing between two plates is 2 mm, the explosive density is 850 kg/cm^3, the thickness is 9 mm, the optimal collision point movement speed V_c is 2100 m/s, and the optimal collision speed V_p is 470 m/s.

2) Boundary effect can be observed near the initiation point. With the explosive welding further proceeding, the bonding interface is gradually transformed from a straight bonding zone to a corrugated bonding zone, and whirlpool structures appear.

3) The shear strength at the interface of N6/45# composite plate after explosive welding reaches 325.5 MPa, indicating that the composite plate has high bonding strength. At the bonding interface, the thickness of the diffusion layer is 20 μm, which is beneficial to the metallurgical bonding at the explosive welding interface.

4) The interface waves obtained by numerical simulation are consistent with the experiment results. The simulation results show that the velocity and plastic deformation of the characteristic points are highly consistent with the experiment results, which also proves that the welding quality of N6/45# composite plate after explosive welding is very high.

References

1 Jandaghi R M, Saboori A, Khalaj G *et al*. *Metals*[J], 2020, 10(5): 634

2 Liang H L, Luo N, Chen Y L *et al*. *Journal of Materials Research and Technology*[J], 2022, 18: 564

3 Zeng X Y, Li X Q, Li X J *et al*. *The International Journal of Advanced Manufacturing Technology*[J], 2019, 104(5–8): 2607

4 Parchuri P, Kotegawa S, Yamamoto H *et al*. *Materials & Design*[J], 2019, 166: 107610

5 Wang Xuezhen, Lu Guangming, Jiang Shan *et al*. *Materials China*[J], 2023, 42(5): 431 (in Chinese)

6 Liu Xianghong, Li Qinqin, Gao Huixian *et al*. *Titanium Industry Progress*[J], 2022, 39(2): 12 (in Chinese)

7 Satyanarayan S, Akihisa M, Masatoshi N *et al*. *Journal of Materials Processing Technology*[J], 2018, 267: 152

8 Wang J, Li X J, Yan H H *et al*. *The International Journal of Advanced Manufacturing Technology*[J], 2022, 112(9): 3595

9 Tian X X, Wang Z K, Teng X Y *et al*. *IOP Conference Series: Materials Science and Engineering*[J], 2020, 811: 012013

10 Li X J, Mo F, Wang X H *et al*. *Science and Technology of Welding and Joining*[J], 2012, 17(1): 36

11 Wu X M, Shi C G, Gao L *et al*. *Rare Metal Materials and Engineering*[J], 2023, 52(4): 1272

12 Yang Rongzun. *Transactions of the China Welding Institution*[J] 2006, 27(12): 54 (in Chinese)

13 Gong Pengtao, Lin Peng, Meng Lingjian *et al*. *Rare Metal Materials and Engineering*[J], 2022, 51(11): 4258 (in Chinese)

14 Zhang B, Zhu L L, Wang K S *et al*. *Rare Metals*[J], 2015, 39(5): 406

15 Jia Z, Wei B L, Sun X *et al*. *Transactions of Nonferrous Metals Society of China*[J], 2022, 32(10): 3259

16 Cai D Y, Xiong L Y, Liu W C *et al*. *Materials Characterization*[J], 2007, 58(10): 941

17 Walsh M J, Shreffler G R, Willig J F. *Journal of Applied Physics*[J], 1953, 24(3): 349

18 Cowan R G, Bergmann R O, Holtzman H A. *Metallurgical and Materials Transactions B*[J], 1971, 2(11): 3145

19 Blazynski T Z. *Explosive Welding, Forming and Compaction*[M]. Berlin: Springer Science & Business Media, 1992

20 Cui Y, Liu D, Fan M Y *et al*. *Materials Science and Technology*[J], 2020, 36(4): 425

21 Stivers S W, Wittman R H. *Proceeding of 5th International Conference of High Energy Rate Fabrication*[C]. Denver: University of Denver Research Institute, 1975: 16

22 Li Yan, Li Yanbiao, Liu Cuirong *et al*. *Welding*[J], 2021(9): 10 (in Chinese)

23 Wronka B. *Journal of Materials Science*[J], 2010, 45(13): 4078

24 Zhang Jinmin, Yue Zonghong, Guo Haixia *et al*. *Special Casting and Nonferrous Alloy*[J], 2007(9): 670 (in Chinese)

25 Jiang Chao, Long Weimin, Feng Jian *et al*. *Welding*[J], 2021(9): 22 (in Chinese)

26 Zhou Q, Feng J R, Chen P W. *Materials*[J], 2017, 10(9): 984

27 Abhishek B, Siddharth J, Kanchan K *et al*. *Welding International*[J], 2022, 36(8): 455

28 Poeuf S, Genetier M, Lefrançois A *et al*. *Propellants, Explosives, Pyrotechnics*[J], 2018, 43(11): 1157

29 Wang X, Zheng Y Y, Liu H X *et al*. *Materials & Design*[J], 2012, 35: 210

30 Sun Z R, Shi C G, Xu F *et al*. *Materials & Design*[J], 2020, 191: 108630

爆炸焊接N6/45#复合板的数值模拟与实验分析

张文斌[1]，杨海娟[1]，刘翠荣[1,2]，李　岩[1,2]，史爱尊[1]
(1. 太原科技大学 材料科学与工程学院，山西 太原 030024)
(2. 山西师范大学 现代文理学院 转设筹备处，山西 临汾 041000)

摘　要：为降低使用成本，充分发挥镍材优异的耐腐蚀性能优势，选用厚度1 mm的纯镍N6作为复板、3 mm厚的中碳钢45#作为基板进行爆炸焊接试验。通过爆炸焊接窗口计算出了各动态参数，采用金相光学显微镜和扫描电镜对界面结合形貌和元素进行分析，通过拉剪试验测试复合板力学性能，并借助AUTODYN模拟了爆炸焊接过程。结果表明，爆炸点附近存在边界效应，沿着爆炸焊接方向结合界面由平直状转变为稳定的波状界面，界面附近元素扩散层厚度为20 μm，波状的扩散层增大了结合面积，有利于冶金结合，复合板剪切强度达到325.5 MPa。数值模拟结果表明，界面形貌与试验得到的界面形貌具有一致性。模拟结果表明特征点的速度和塑性变形程度与实验结果基本吻合。

关键词：爆炸焊接；N6/45#复合板；焊接窗口；数值模拟

作者简介：张文斌，男，1997年生，硕士，太原科技大学材料科学与工程学院，山西 太原 030024，E-mail：S202114210098@stu.tyust.edu.cn